Microsyst Technol (2008) 14:307–314
DOI 10.1007/s00542-007-0430-1

TECHNICAL PAPER

Development of a novel type of microrobot for biomedical application

Shuxiang Guo · Qinxue Pan · Mir Behrad Khamesee

Received: 1 February 2007 / Accepted: 23 July 2007 / Published online: 15 September 2007
© Springer-Verlag 2007

Abstract This paper proposes a new type of microrobot that can move along a narrow area such as blood vessels which has great potential for application in microsurgery. Also, the development of a wireless microrobot that can be manipulated inside a pipe by adjusting an external magnetic field has been discussed. The model microrobot utilizes an electromagnetic actuator as the servo actuator to realize movement in biomedical applications. The structure, motion mechanism, and evaluation characteristic of motion of the microrobot have been discussed, and the directional control can be realized via the frequency of the input current. The moving experiments have been carried out in branching points in the horizontal direction, and the moving speed of the robot has been measured in vertical direction by changing frequency. Based on the results, the microrobot has a rapid response, and it can clear out dirt which is adhering to the inner wall of pipe. This microrobot will play an important role in both industrial and medical applications such as microsurgery.

S. Guo · Q. Pan (✉)
Kagawa University, 2217-20, Hayashi-cho,
Takamatsu, 761-0396 Kagawa, Japan
e-mail: s07d506@stmail.eng.kagawa-u.ac.jp

S. Guo
e-mail: guo@eng.kagawa-u.ac.jp

M. B. Khamesee
University of Waterloo,
200 University Avenue West,
N2L3G1 Waterloo, ON, Canada
e-mail: khamesee@mecheng1.uwaterloo.ca

1 Introduction

Microsurgery in blood vessels is expected to become an increasingly popular medical practice. Several kinds of microrobots have been developed for various purposes owing to advances in precise process technology, and further progress in this field is expected. One use of a microrobot is as a tool in very small spaces, and in medical practice, their use avoids the need for dismantling and reassembling. In medical and industrial applications, a new type of microrobot in a pipe has urgently been needed (Fearing 1992; Osada et al. 1992; Guo et al. 2005). The microrobot is installed with sensing and actuating elements, and can move smoothly in water or aqueous medium, making it suitable for pipe inspection and microsurgery of blood vessels.

A direct conversion of chemical activity to mechanical activity has been pursued by many researchers in order to achieve high efficiencies. Among various forms of locomotion, the forward swimming motion of a fish in water has been the subject of interest for zoologists, marine biologists, and engineers. Advantages of the wavy motion of the swimming body as compared to a mechanical propeller used in artificial swimming structures are numerous and can be attributed to its high energy-conversion efficiency, noiseless propulsion, and utilization of the energy of the surrounding medium. Mechanical swimming structures such as those replicating undulatory motion by means of linkages and other interfacing parts face the same problems as propellers, which have low efficiencies and excessive thermal energy generation. Recently, several types of microrobots in pipes using SMA, PZT, and polymer actuators have been reported (Fukuda et al. 1995; Sendoh et al. 2000; Guo et al. 2003). However, some problems exist, such as compactness, low response, and safety in water.

In this paper, a novel type of microrobot in a pipe is being presented, which has flexibility, wireless control, good response, and safe application in the body. Up to now, several kinds of microrobots in pipe have been developed (Fukuda et al. 1995; Sendoh et al. 2000; Guo et al. 2003). However, the power supply and the friction power with the inner wall were typically problematic in this research. It has been reported that a novel prototype model of a microrobot utilizes an electromagnetic actuator as the servo actuator to realize motion (Guo et al. 2002, 2003). With this paper, we are presenting a microrobot, which has a moving fin driven by a permanent magnet is controlled via frequency adjustment of the alternate magnetic field. Here an improved prototype of a microrobot is proposed. Experiments were carried out, and operating characteristics were evaluated both in the horizontal direction and in the vertical direction. The proposed microrobot can correspond with the dirt adhering to the inner wall; it is capable of long-distance travel, even in vertical directions, and its speed can be easily controlled via frequency adjustment of the alternate magnetic field.

2 Structure of the microrobot in a pipe

Figure 1 shows the structure of a fin-driven type of microrobot. This microrobot is composed of a streamlined main body made of wooden and styrol materials; the fin consists of a polyimide film sheet. The prototype of the microrobot is shown in Fig. 2. A permanent magnet which be shown in Table 1, and six kinds of driving fin are shown in Table 2.

In Fig. 3, the control and locomotion of the microrobot are described. When current flows through a coil, an alternate magnetic field parallel to the promotion advance direction is applied; this movement exerts force arising from a permanent magnet, which rotates and vibrates, and causes rotation and vibration of the fin connected to it. The structure is simple and does not require wires.

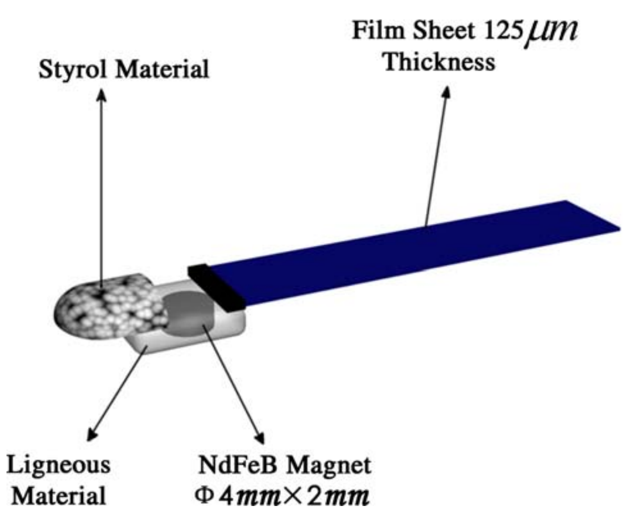

Fig. 1 Structure of the fishlike microrobot

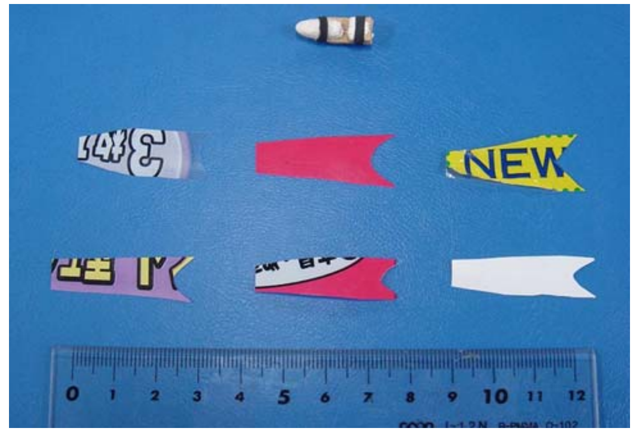

Fig. 2 Prototype of microrobot

3 Motion mechanism of the microrobot

3.1 Kinematics of the driving fin

According to biomechanics theory, a large undulatory motion near a fishtail results from an anguilliform mode of swimming, which involves most of the fish's body in an undulating or wavy motion.

Rosen (Sendoh et al. 2000) was among the first to explain the kinematics of motion in a simple carangiform fish through his observations using simple hydrodynamic forces and phenomena. He described the creation and evolution of vortices generated by the anterior half of the body (head and after-head of the fish) and cited them as the main reason for

Table 1 The parameter of the magnet

Size (mm)	Magnetic field (B) (mT)	Weight (g)	Magnetism (kg)
$\phi 4 \times 2$	330	0.19	0.35

Table 2 Measurements of the fin

	Length A (mm)	Width B (mm)	Thickness C (mm)
Robot1	40	10	0.125
Robot2	40	10	0.5
Robot3	40	10	1
Robot4	40	15	0.125
Robot5	40	15	0.5
Robot6	40	15	1

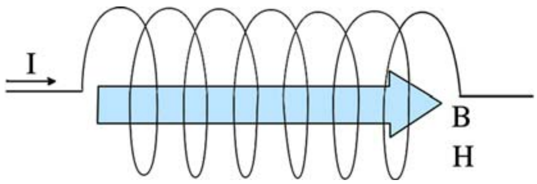

Fig. 3 Solenoid features

its propulsion through water. The fish further uses these vortices created by the last two-thirds of its body (after-half) to propel itself forward by thrusting its body against the seemingly fixed vortices and utilizing their rotational energy. This is known as the "vortex peg hypothesis." The fish produces no net backward moving stream of water when swimming at constant speed. Only when the fish accelerates or turns around, is a trailing current created. The trail created by the fish is a system of large, slow-spiraling vortices. The trail consists of a single row of vortices with direction of rotation alternating from one vortex to the next. This row follows the path of the fish's head. The concave side of each flexural wave of the body of the fish contains one vortex. All main vortices are in line with and follow the fish's direction of travel. For a scaled fish, the mechanism of propulsion is even more complex since the convex portion of the body in effect has open scales that act as small paddles on the side of the fish, further pushing against the vortices to propel the fish forward.

3.2 Motion mechanism

The microrobot has a fin driven by an alternate magnetic field; the fin is fixed on a permanent magnet. When current flows through the solenoid, a magnetic field is generated. Directions of the current and magnetism are shown in Fig. 4 the following equation is obtained:

$$\overrightarrow{B} = \mu_0 \overrightarrow{H} = \mu_0 n \overrightarrow{I} \tag{1}$$

To calculate the force of the magnet and the moment of the magnetic field; the analyzing force graph is shown in Fig. 4. Equations 1 and 2 can be obtained as well.

$$m = qr \tag{2}$$

$$\overrightarrow{T} = \overrightarrow{m} \times \overrightarrow{H} \tag{3}$$

Here, B is the magnetic flux density; H is the magnetic field strength; μ_0 is the permeability of vacuum; n is number of turns in unit length; I is the current in coil; T is the magnetic torque; m is the magnetic moment; q is a magnetic charge; r is the distance between positive and negative charges.

According to the equation above, if the current will be increased, the magnetism and torque will increase. If the torque becomes large, displacement of the tail will increase, and the propulsive force will become larger.

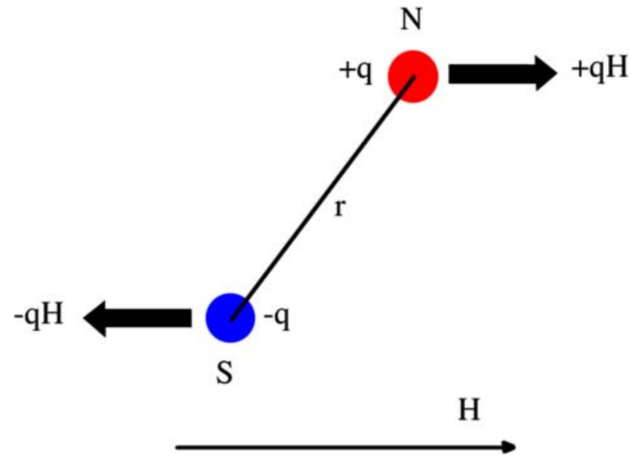

Fig. 4 Magnetism of the microrobot

However, when an alternate magnetic field parallel to the direction of advance is applied, movement due to an impelling force arising from a permanent magnet rotates and vibrates the connected fin as shown in Fig. 5. The propulsive force is the sum of the drag force vectors in the direction of movement as in Eq. 4. The speed of the microrobot can be controlled by adjusting the frequency of the input current:

$$P = -\frac{1}{2} C_d \rho A |V_k| V_k \tag{4}$$

In this case, C_d is a drag coefficient based on wetted surface area A, and ρ is the density of the fluid.

4 Evaluation of fin characteristics

4.1 Measurement system of a driving fin

A computer can control the electric current in the long solenoid coil, and the electrical current is measured by a galvanometer. The bending displacement of a fin at the

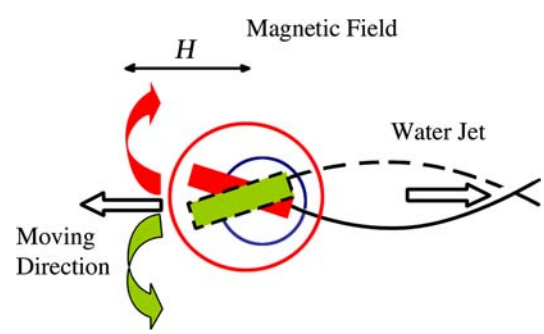

Fig. 5 Driving mechanism of the microrobot

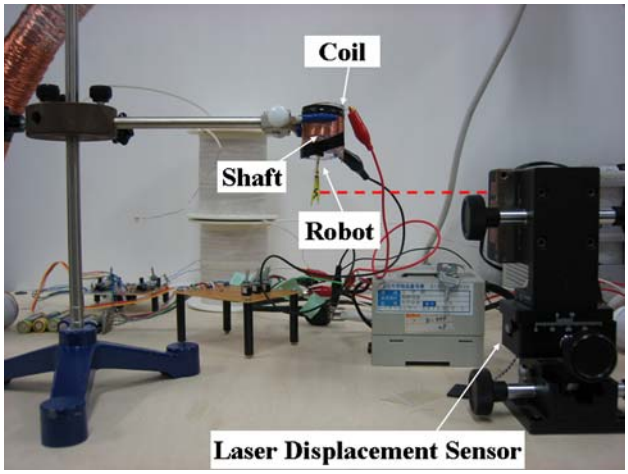

Fig. 6 Measurement system for displacement of the fin

front end is measured by a laser displacement sensor. The bending amplitude of the fin can be obtained; the measurement system is shown in Fig. 6.

4.2 Characteristic evaluation of a driving fin

Using the measurement system shown in Fig. 6, the following characteristics of a fin are measured. First, measure the maximum displacement of a fin at the front end by changing the frequency of current from 5 to 60 Hz. Figure 7 shows the experimental results of the driving fins by frequency of input current. Maximum displacement is obtained when the frequency is 30 Hz. According to selected experimental results, the natural frequency of the driving fin can be obtained. Characteristics of the driving fin using a cantilever model can be evaluated. The movement equation of horizontal vibration of a cantilever beam can be obtained from Eq. 5:

$$EI\frac{\partial^4\omega}{\partial\chi^4} + \rho A\frac{\partial^2\omega}{\partial t^2} = 0. \tag{5}$$

If the conditions of fixed-freedom are substituted for the general solution of Eq. 5, Eq. 6 can be obtained:

$$1 + \cos\alpha \cdot \cosh\alpha = 0. \tag{6}$$

In this formula, α is the characteristic value. Using equation (7), the natural frequency of a driving fin can be calculated as

$$f_i = \frac{\alpha_i}{2\pi} \cdot \frac{1}{l^2} \cdot \sqrt{\frac{EI}{\rho A}} \tag{7}$$

where f_i is the natural frequency of the driving fin, E is the Young's modulus of the fin, I is the secondary section

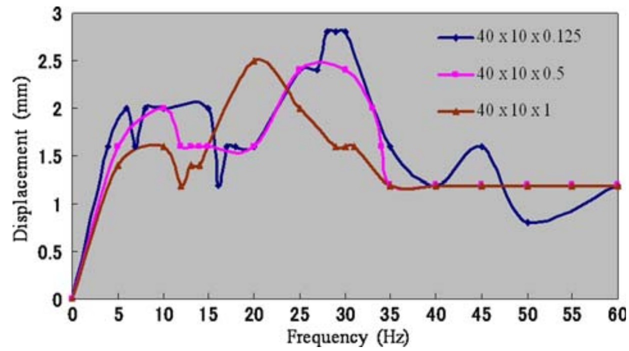

Fig. 7 Displacement of the fin by frequency

moment, ρ is the density of the fin, A is the cross-sectional area, l is the length of the fin, and α_i is the characteristic value of the fin.

5 Motion of the microrobot

The propulsive force must be considered, resistance force, and flotage in the vertical direction in order to realize work and movement by the microrobot in a pipe or a coil. In addition, the effects of the microrobot's weight on motion are significant. These factors should be evaluated at the point of motion.

5.1 Analysis of the motion state

According to the motion state in a pipe, the appropriate functions can be obtained as follows.

In the horizontal direction:

$$Ma = F - F_D \tag{8}$$

Rising in the vertical direction:

$$Ma = F - F_D - Mg + \rho gV \tag{9}$$

Falling in the vertical direction:

$$Ma = F - F_D + Mg - \rho gV \tag{10}$$

$$F_D = C_D A \frac{\rho u^2}{2} \tag{11}$$

Where M is the mass of the microrobot, a is acceleration, F is the propulsive force, F_D is the resistance force, ρ is the density of the fluid, A is the maximum cross-sectional area of the moving object, and u is the velocity of the object. This study focuses on how to obtain propulsive forces without wires or cables.

5.2 Moving forward in the horizontal direction

To evaluate the motion of the microrobot described in this paper, experiments in horizontal directions has been carried out. Accordingly, it is found that the fishlike microrobot can move steadily and safely, and can negotiate bifurcations or branching points. The state of moving in the pipe in horizontal directions is shown in Fig. 8. Here, we separated the pipe into three sections as A, B, C; signals control each section of the pipe. When we have the microrobot turn left, we can switch on the current on part A and B, in the same way, when we have the microrobot turn the right, the current of part A and C will be switch on, in addition, by change the frequency of input current, the directional control can be carried out, respectively.

5.3 Upward motion in a pipe

The microrobot is shown in Fig. 1 with a permanent magnet built in. When designing the microrobot, the relationship between flotage and deadweight should be considered so that it can be suspended in water without outside forces. To drive the microrobot by an alternate magnetic field with a coil, the direction of magnetization in a permanent magnet is vertical and related to the height of a pillar. To verify the performance of the microrobot, the experiments within a 1,000-mm-tall pipe filled with water have been carried out. The locomotion mechanism is very effective in such a pipe. The state of upward locomotion by the microrobot is shown in Fig. 9a.

5.4 Analysis of the state of stopping in pipe

Several studies on underwater microrobots or fishlike microrobots in pipes have recently been completed. Much work has been done in the area of matching propulsion requirements to an optimal propeller. However, some of these studies have ignored the need for discretional stopping, in particular, the ability to stop in the vertical direction without a wire. If the microrobot is to be used widely in biology and chemistry, it is necessary that focus on its capability to cease motion.

In this report, a method of stopping motion has been introduced. The magnetic robot can move upward and downward freely by changing the frequency. However, according to the theory of motion, in order to obtain alternations of the magnetic field, an alternating current is required. Under such conditions, a permanent magnet can regulate rotation and vibration.

Figure 9b shows that by changing the alternating current into direct current, the microrobot can be asked to stop vibrating and repose anywhere. A parallel magnetic field will be running simultaneously in the same direction in the solenoid. The magnet turns in a parallel direction as a result of the magnetic torque M, shown in Fig. 10. Because of the torque, force F is vertical to the head. As a component of the force, the pressure F_N is vertical to the inner wall. So the biggest static friction of the head $f_{\max}$ equals $2F_N \times f$, where f is the coefficient of friction, shown in Eqs. 12–15. When resistance from the weight or fluid is less than $f_{\max}$, the robot no longer depends on the friction of the inner wall.

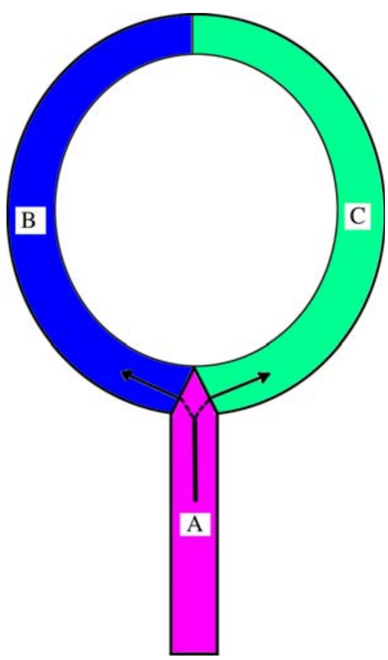

Fig. 8 Microrobot movement in a horizontal pipe

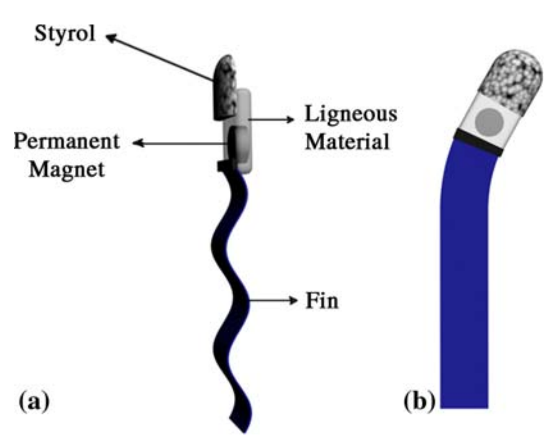

Fig. 9 **a**, **b** Microrobot movement in a vertical pipe

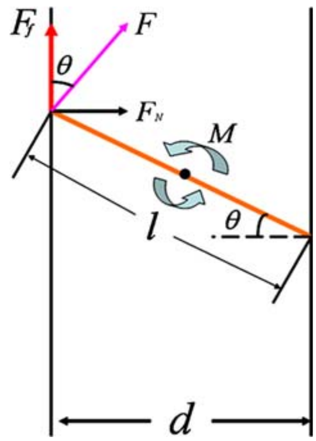

Fig. 10 Stopping model in a vertical pipe

$$M = Fl \tag{12}$$

$$F_N = F\sin\theta \tag{13}$$

$$\theta = \arccos\frac{d}{l} \tag{14}$$

$$f_{\max} = 2F_N f = 2\frac{Mf\sqrt{l^2 - d^2}}{l^2} \tag{15}$$

6 Experimental results

In this paper, experiments on the prototype microrobot using a measurement system have been conducted. As outlined in Fig. 11, the propulsive forces for various frequencies were measured using a laser displacement sensor, an electric balance, and a copper beam. The copper beam was soft enough to bend under the propulsive force. The electric balance was used to evaluate the propulsive force.

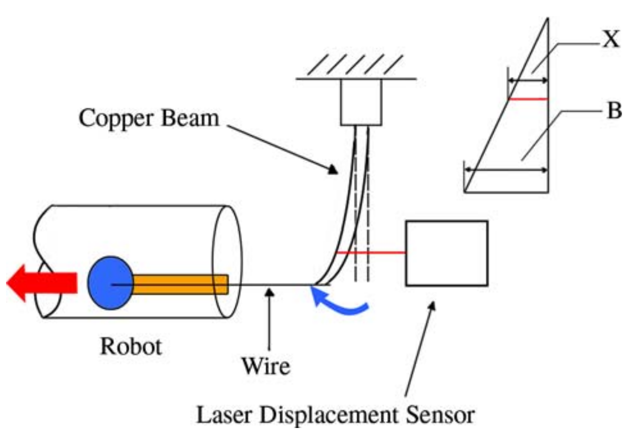

Fig. 11 Measurement of propulsive force

Results of bending the copper beam with the propulsive force are shown in Fig. 12. Based on the experimental results, a calibration calculation has been carried out, and obtained the relationship between the propulsive force and bending displacement of the copper beam, as shown in Eq. 16:

$$F = \frac{1}{0.4394} \times x \approx 2.276x \tag{16}$$

where x is the bending displacement of the copper beam measured by a laser sensor and F is the propulsive force.

Based on Eq. 16, the propulsive force of the microrobot can be obtained. By changing the input electric currents to a sine signal, triangle signal, and pulse, the propulsive forces for various frequencies are measured as shown in Fig. 13. Based on the experimental results, it is very easy to control the propulsive force of the microrobot by changing the frequency of the input current.

The running experiment of the prototype microrobot has been carried out by using a measurement system shown in Fig. 14. By changing the frequency of input current from 0 to 80 Hz in horizontal direction and 0 to 30 Hz in vertical direction, the maximum moving speed in horizontal direction 63 mm/s can be obtained which is shown in Fig. 15. And the maximum moving speed 40 mm/s in vertical direction has been obtained as shown in Fig. 16.

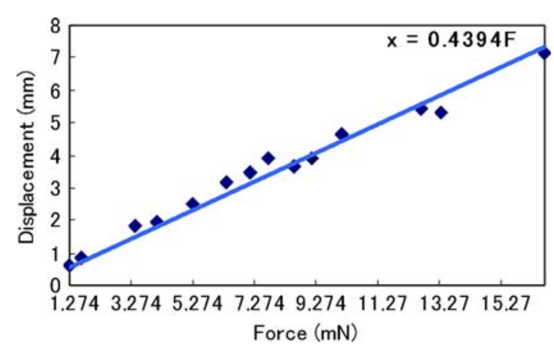

Fig. 12 Calibration of the copper beam

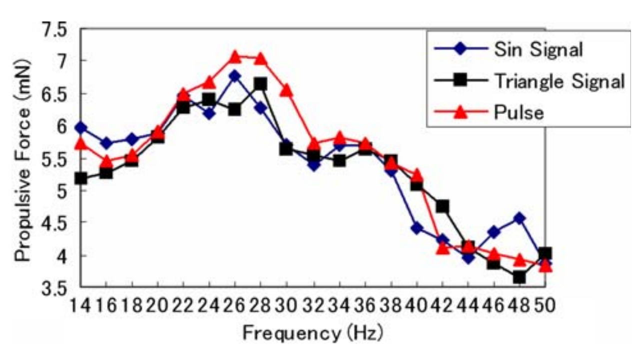

Fig. 13 Experimental results of propulsive force

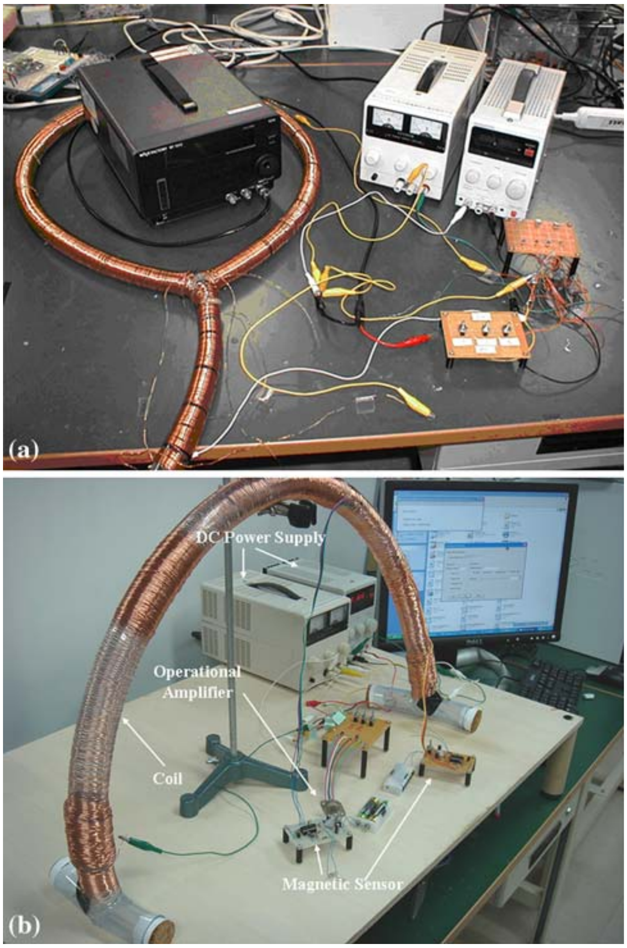

Fig. 14 a Experiment in horizontal directions. **b** Experiment in vertical directions

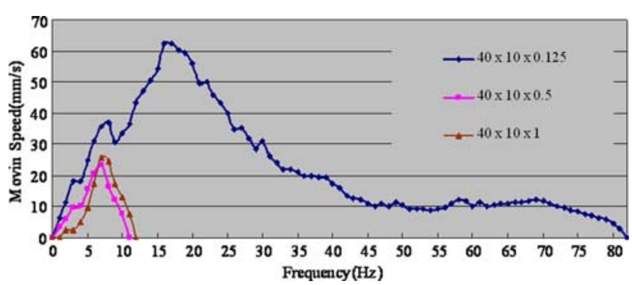

Fig. 15 Experimental results of horizontal speed

According to the experimental results, it is found that the thickness and width of the fin of the robot has an influence on speed of the robot.

However, the measurement of the displacement of the fin has been introduced at the front page in this paper, the maximum displacement which can be obtained in the air when the frequency is about 30 Hz, but here the maximum speed that has been obtained in the water as the frequency is 20 Hz. It means that the fluid has an influence on the fin

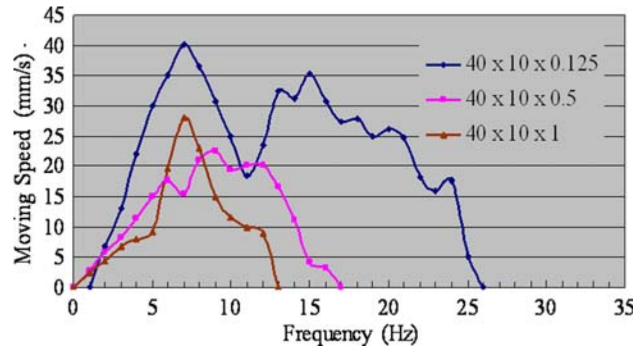

Fig. 16 Experimental results of speed in vertical directions

of the microrobot. So some important factors like as viscosity and fluid density must be considered in the following research.

7 Conclusions

In this paper, a novel type of microrobot in pipe has been proposed. We also discussed the structure, motion mechanism, and evaluated the characteristic of motion for the microrobot.

Firstly, we designed the structure of microrobot with two sorts of driving fin in different thickness and carried out experiments on measurement of displacement of the driving fin. According to the experimental results, the maximum displacement 3 mm can be obtained. We can determine what size is the optimal for the driving fin.

Secondly, we evaluated the characteristic of motion of the microrobot. We carried out the experiment of moving forward and turning at branching points in horizontal direction, going upward and stopping motion in vertical direction. Based on the experimental results, we realized the motion control of the microrobot both in horizontal and vertical direction.

Thirdly, we measured the propulsive forces with various frequencies of input current by utilizing the laser displacement sensor. Based on the experimental results, a calibration calculation has been carried out, and obtained the relationship between the propulsive force and bending displacement of the copper beam.

In the future, we will deal with optimizing the design of the microrobot and efficiency of energy supply by wireless. We also try to develop a robot to move along a pipe with various branching points such as blood vessel. Moreover, we will realize detecting and controlling the position of the microrobot. Therefore, this kind of microrobot with the application of in-pipe inspections, operation in microenvironment and microsurgery of blood vessels will be very useful to industrial and medical fields.

References

Anderson JM, Triantafyllou MS, Kerrebrock PA (1997) Concept design of a flexible-hull unmanned undersea vehicle. In: Proceedings of the international offshore and polar engineering conference, pp 82–88

Barrett D, Yue DKP, Grosenbaugh, Wolfgang MJ (1999) Drag reduction in fish-like locomotion. J Fluid Mech 392:183–212

Bone Q, Marshall NB (1982) Biology of fishes. Blackie and Son Limited, London, 167 p

Domenici P, Blake RW (1997) The kinematics and performance of fish fast-start swimming. J Exp Biol 200(8):1165–1178

Fearing L (1992) Micro structures and micro actuator for implementing submillimetres robots, precision sensors, actuators and systems. Kluwer, Dordrecht, pp 39–72

Fukuda T, Kawamoto A, Arai F, Matsuura H (1994) Mechanism and swimming experiment of micro mobile robot in water. Proc IEEE Int Conf Robot Autom 1:814–819

Fukuda T, Kawamoto A, Arai F, Matsuura H (1995) Steering mechanism of underwater micro mobile robot. Proc IEEE Int Conf Robot Autom 1:363–368

Guo S, Pan Q (2007) Mechanism and control a novel type of microrobot for biomedical application. In: Proceedings of the 2007 IEEE international conference on robotics and automation, pp 187–192, Roma, Italy

Gray J (1936) Studies in animal locomotion. VI. The propulsive powers of the dolphin. J Exp Biol 13:192–199

Guo S, Pan Q (2006) Design and control of a novel type of microrobot moving in pipe. In: Proceedings of the 2006 IEEE international conference on mechatronics and automation, pp 649–653, China

Guo S, Fukuda T, Kosuge K, Arai F, Oguro K, Negoro M (1995) Micro catheter system with active guide wire. In: Proceedings of the 1995 IEEE international conference on robotic and automation, vol 1, Nagoya, Japan, pp 79–84

Guo S, Fukuda T, Kato N, Oguro K (1998) Development of underwater micro robot using ICPF actuator. In: Proceedings of the 1998 IEEE international conference on robotics and automation, Belgium, pp 1829–1834

Guo S, Sugimoto K, Hata S, Su J, Oguro K (2000) A new type of underwater fish-like micro robot. In: Proceedings of the 2000 IEEE international conference on intelligent robotics and systems, Kagawa, Japan, pp 867–862

Guo S, Fukuda T, Asaka K (2002) Fish-like underwater micro robot with 3 DOF. In: Proceedings of the 2002 IEEE international conference on robotics and automation, Washington, DC, pp 738–743

Guo S, Sasaki Y, Fukuda T (2002) A fin type of microrobot in pipe. Proceedings of the 2002 international symposium on micro machine and human science (MHS' 22), Nagoya, Japan, pp 93–98

Guo S, Fukuda T, Asaka K (2003) A new type of fish-like underwater microrobot. IEEE ASME Trans Mechatron 8(1):35–40

Guo S, Sasaki Y, Fukuda T (2003) A new kind of microrobot in pipe using driving fin. In: IEEE/ASME international conference on advanced intelligent mechatronics (AIM 2003), Kobe, Japan, pp 667–702

Guo S, Sakamoto J, Pan Q (2005) A novel type of microrobot for biomedical application. In: IEEE/RSJ international conference on intelligent robots and systems (IROS2005), Canada, pp 2265–2270

Guo S, Pan Q, Khamesee MB (2006) Development of a novel type of microrobot for biomedical application. ASME/JSME joint conference (MIPE 2006), Santa Clara, CA, USA

Guo S, Pan Q, Zhang W (2006) Characteristics of the microrobot moving in the vertical pipe. Proceedings of the 6th World Congress on Control and Automation, pp 9282–9286, China

Harper KA, Berkemeier MD, Grace S (1998) Modeling the dynamics of spring-driven oscillating-foil propulsion. IEEE J Ocean Eng 23:285–296

Hirose Y, Shiga T, Okada A, Kurauchi T (1992) Gel actuators driven by an electric field. In: Proceedings of the 3rd international symposium on micro machine and human science, pp 21–26

Laurent G, Piat E (2001) Efficiency of swimming microrobots using ionic polymer metal composite actuators. In: Proceedings of 2001 IEEE international conference on robotics and automation, pp 3914–3919

Maddock L, Bone Q et al (1994) Mechanics and physiology of animal swimming. Cambridge University Press, Cambridge

Mojarrad M, Shahinpoor M (1997) Biomimetic robot propulsion using polymeric artificial muscles. In: Proceedings of the 1997 IEEE international conference on robotics and automation, New Mexico, USA, pp 2152–2157

Oguro K, Asaka K, Takenaka H (1993) Polymer film actuator driven by a low voltage. In: Proceedings of the 4th international symposium on micro machine and human science, Japan, pp 39–40

Osada Y, Okuzaki H, Hori H (1992) A polymer gel of electrically driven moiety. Nature 355:242–244

Pan Q, Guo S (2006) A novel type of microrobot moving in the vertical pipe. In: The 24th annual conference of the robotics society of Japan, 2G22, Japan

Sendoh M, Yamazaki A, Ishiyama K (2000) Wireless controlling of the swimming direction of the spiral-type magnetic micro-machines. Trans IEEE Jpn 120-A:301–306

Sfakiotakis M, Lane DM, Davies JBC (1999) Review of fish swimming modes for aquatic locomotion. IEEE J Ocean Eng 24:237–252

Tadokoro S, Takamori T et al (1998) Development of a distributed actuation device consisting of soft gel actuator elements. In: Proceedings of 1998 IEEE international conference on robotics and automation, Leuven, Belgium, pp 2155–2160

Tadokoro S, Yamagami S et al (1999) Multi-DOF device for soft micromanipulation consisting of soft gel actuator elements. In: Proceedings of the 1999 IEEE international conference on robotics and automation, Detroit, MI, USA, pp 2177–2182

Tadokoro S, Yamagami S, Takamori T (2000) An actuator model of ICPF for robotic applications on the basis of physicochemical hypotheses. In: Proceedings of the 2000 IEEE international conference on robotics and automation, Seoul, Korea, pp 1340–1345

Triantafyllou MS, Triantafyllou GS (1995) An efficient swimming machine. Sci Am 272(3):64–70